Talanta 81 (2010) 1109–1115

Contents lists available at ScienceDirect

Talanta

journal homepage: www.elsevier.com/locate/talanta

A cold plasma dielectric barrier discharge atomic emission detector for atmospheric mercury

Mahitti Puanngam[a,b], Shin-Ichi Ohira[a], Fuangfa Unob[b], Jian-Hua Wang[c], Purnendu K. Dasgupta[a,*]

[a] Department of Chemistry and Biochemistry, The University of Texas at Arlington, 700 Planetarium Place, Arlington, TX 76019-0065, United States
[b] Department of Chemistry, Faculty of Science, Chulalongkorn University, Bangkok 10330, Thailand
[c] Research Center for Analytical Sciences, Northeastern University, Box 332, Shenyang 110004, China

ARTICLE INFO

Article history:
Received 3 January 2010
Received in revised form 31 January 2010
Accepted 1 February 2010
Available online 6 February 2010

Keywords:
Mercury
Atomic emission
Dielectric barrier discharge
Preconcentration on gold
Airborne mercury

ABSTRACT

An automated atmospheric elemental mercury analyzer based on the dielectric barrier discharge (DBD) atomic emission technique was developed. The instrument is based on a gold-on tungsten coiled filament preconcentrator fashioned from commercial quartz-halogen lamps, a DBD excitation source and a radiation detector. An in-house program provided system control and data collection. Several types of radiation detectors, e.g., charge coupled device (CCD) array spectrometers, photomultiplier tubes (PMTs) and phototube (PT) are investigated. An argon plasma provided better performance than a nitrogen plasma. With ~0.88 standard liters per min sampling rate and preconcentration for 2 min, the estimated (S/N = 3) detection limit was 0.12 ng/L (Hg^0), the linear range extended at least to 6.6 ng Hg/L. Typical RSD values for determination at the single digit ng/L level ranged from 2.8 to 4.9%. In 19 separate calibrations conducted over 7 days, the calibration slope had a standard error of 1%. The system was applied to the determination of atmospheric mercury in two different locations.

1. Introduction

Mercury, "quicksilver", has been an enigmatic metal since antiquity. Mercury has been widely used because of its unique properties. The recognition that it is an extremely toxic metal, both as the element and its compounds, has resulted in a drastic reduction of its use in recent decades, both industrially and otherwise. But the legacy of that use is its wide dispersion, from the air to the sediments and even in biota. Any review of mercury and its consequences is quite beyond the scope of any single article, a recent search of the Web of Science database over the period 1965–2010 yields 130+ articles in which "mercury" and "review" both appear in the title.

There are several sensitive and robust measurement methods for mercury [1]; the ability to generate the analyte as the element in the vapor phase and the ability to selectively preconcentrate (and thermally release) Hg on/from gold aid trace analysis. Indeed, because there are so many methods and techniques applied for the measurement/speciation of mercury and its compounds (dialkyl, monoalkyl, inorganic Hg (in 0, +1 and +2 oxidation states), gaseous, reactive gaseous mercury (largely meaning gaseous inorganic Hg(II)), particulate mercury (any form of Hg, associated with particles or aerosols)), there are few comprehensive reviews on the analytical chemistry of mercury; the last one is more than a decade old [2]; other/more recent reviews have only a narrow focus [3–5]. The chemistry of mercury is not always intuitive: the loss of elemental mercury by volatilization can be prevented by covering mercury with an oxidant solution, e.g., acidic permanganate. Interestingly, the loss of mercury by volatilization through a layer of acid occurs at a measurable rate and quixotically, the loss rate is very substantially greater through a layer of HNO_3, compared to HCl or H_2SO_4 [6].

The cycling of mercury through the atmosphere is a major vector for mobilizing mercury in the environment; the atmospheric chemistry of mercury has been concisely reviewed [7]. The majority (~95%) of mercury in the atmosphere is in the elemental (Hg^0) form. Atmospheric residence time of mercury was believed to be from 1 to 2 years but more recent work suggests it may be just a few months [8], which nevertheless is enough for mercury emitted in any region to be dispersed globally. In the wake of increased coal combustion there is greater concern about mercury emissions (mercury content of US coal ranges from 2.1 to 15.7 g per GJ of heat generation [9]) and a greater need for widely applicable measurement of elemental Hg in an inexpensive manner. Particularly a portable device able to measure ambient background levels will be highly desirable.

A variety of options are available for the measurement of gaseous Hg^0. In almost all cases some preconcentration is needed to measure background levels. Gold not only takes up mercury efficiently, the resistivity of gold changes [10] upon mercury

* Corresponding author. Tel.: +1 817 272 3171.
E-mail address: dasgupta@uta.edu (P.K. Dasgupta).

0039-9140/$ – see front matter © 2010 Elsevier B.V. All rights reserved.
doi:10.1016/j.talanta.2010.02.005

uptake enabling thin gold film based resistive sensors for mercury [11]. Atomic spectrometry, especially emission spectrometry, is one of the most sensitive techniques to determine the Hg^0. This includes atomic fluorescence [12], inductively coupled plasma [13], microwave induced plasma [14] and glow discharge spectrometry [15], etc. Very recently Yu et al. [16] and Zhu et al. [17] independently introduced dielectric barrier discharge (DBD) plasma spectrometry. The DBD or silent discharge is non-thermal plasma generated between two electrodes in the presence of at least one dielectric barrier in the current flow path [18]. Both previous papers using DBD-discharge to measure Hg dealt with solution phase Hg; Hg^0 was liberated from a purged solution as a pulse by the addition of a reducing agent. There are several ways to preconcentrate mercury from solution but the method is sufficiently sensitive to not need preconcentration in most cases. One of us (JHW) was the senior author of the first DBD-Hg work [16]. While the present study to optimize the air measurement system involving preconcentration and DBD-based detection was underway, a detailed study on DBD-based detection of Hg by high resolution spectrometry in He or Ar plasmas was independently published [17].

The present paper addresses measurement of Hg^0 in air for which preconcentration is necessary to measure background levels; the most common preconcentration method for Hg^0 is trapping on gold, typically the gold is supported on glass beads [19], silica [20], glass/quartz wool [21], etc. A separate heater is needed to thermally desorb the Hg. We describe a fully automated system for the preconcentration and atmospheric pressure DBD-atomic emission based determination of atmospheric Hg^0. Although a He-plasma may have some advantages [17], we focused on N_2 and Ar plasmas and optimized operating conditions. While a high resolution monochromator can improve S/N, we focused on a portable and inexpensive instrument: we studied the performance of several inexpensive to moderately priced detectors for their relative sensitivities in measuring the mercury emission line at 253.7 nm. Mercury preconcentration was carried out on gold-plated tungsten filaments from a pair of quartz-halogen lamps. This has the advantage of a "built-in" heater and rapid desorption due to a low thermal mass. In addition, preconcentration eliminates the effect of water vapor that was ignored in our previous work [16]. In fact, subsequent studies have shown that plasma instabilities that were believed to be due to Hg introduction (in [16] this was corrected by referencing against a neighboring emission line in the plasma background), is actually due to water vapor that accompanies the sample introduction. In the absence of water vapor no such correction is therefore needed. In addition, it has now been noted that there is a large decrease in intensity of the Hg emission signal in the presence of moisture (>7× for the He-DBD [17]); not having to deal with moisture obviates this issue. System operation was controlled by an in-house program written in Labview software (www.ni.com).

2. Experimental

2.1. Fabrication of the mercury detector

Two PTFE spacers (75 mm × 10 mm × 1 mm) were used as gaskets between two standard microscope glass slides (75 mm × 25 mm × 1 mm) to form a 5-mm wide 1-mm deep flow-through channel across the entire length of the slides where the DBD plasma is generated (see Fig. S1 in Supporting information (SI)). While the assembly is clamped together, silicone adhesive is applied on all sides except the channel openings. One strip each of aluminum foil (50 mm × 10 mm) was affixed on the exterior of each glass slide with black electrical tape and a flat-headed bolt was attached at the gas entrance end of each Al-foil for facile electrical connection by two small pieces of Neodymium magnets (B222, www.kjmegnetics.com). The spacing of the slides is close enough that the oppositely polarized magnet faces hold each other in place. The foils ended 10 mm from the exit of the DBD channel. Disc-shaped end caps/holders were machined from Glass-filled poly(tetrafluoroethylelene) (G-PTFE) for holding the microscope slide discharge assembly. The exit end cap was provided with a threaded axial aperture where a 10 mm dia. fused silica window (NT45-308, www.edmundoptics.com) was placed. Experience showed that at high concentrations mercury may adsorb on this window and this lowers the 254 nm light transmission efficiency dramatically. For high concentration experiments, a flat ring-shaped heater (Polyimide Thermofoil®, HK5186R25.0L12B, www.minco.com, 12.7 mm o.d., 2.4 mm i.d., 0.3 mm thickness) was therefore placed atop the silica window. The heater was powered at 5 V; this was sufficient to maintain the window at ~150 °C. The window was held in place by the adhesive-backed heater. The fiber-optic (P600-025-SR, www.oceanoptics.com, 25 cm long, 600 μm core, SMA 905 terminated, numerical aperture 0.22, acceptance angle 25.4° in air), itself put in a custom-machined insert, held the assembly in place and allowed the detector to view the discharge. The exit end cap further contained a 1/4-28 threaded aperture on the circumference for gas exit. The entrance end cap contained a single 1/4-28 threaded aperture for gas entrance. The discharge voltage was provided by a 100× step-up neon sign transformer (12030P, www.Franceformer.com) and changed by adjusting the input voltage by a variable voltage transformer (3PN1010, www.Stacoenergy.com).

2.2. Mercury calibration source

Elemental mercury was generated from gravimetrically calibrated permeation tubes [22] made in-house from low density polyethylene tubes (80 ± 5 mm × 2.08 mm o.d., 0.51 mm wall thickness). Four separate tubes thus made had average outputs of 12.5 ± 0.9 ng Hg^0/min at 70 ± 0.2 °C; the tube used for most experiments had an output of 11.9 ± 0.7 ng/min over the time it was used. Dilution air was generated by mass flow controllers (Tylan General, Torrance, CA) that were software-controlled by a A/D-D/A card (USB-6009, 14-bit A/D, 12-bit D/A, www.NI.com). All mass flow controllers were calibrated by a NIST traceable primary flow calibrator (Gilibrator, www.sensidyne.com).

2.3. The mercury preconcentrator

The glass envelopes of high-power halogen light bulbs (Hikari JCD 250 W @ 130 V, Fig. S2) were removed at the base by scoring. The non-filament metallic portions were coated with high temperature silicone (automotive gasket grade) to prevent gold from being deposited on areas not directly heated. The filament itself was then coated with gold using in part a plating method for tungsten or molybdenum substrates [23]. Specifically, (a) the filament surface was activated by immersion in 20% H_2O_2 + 0.5 M NaOH for 10 min; (b) the filament was washed thoroughly with DI water; (c) the filament was connected as the (−)ve electrode and a stainless steel wire was connected as the (+)ve electrode and these were dipped into 10 mL of a solution containing 5 g/L of $KAu(CN)_2$ + 50 g/L of Na_2EDTA and placed ~15 mm apart; (d) 1 VDC was applied for 30 min; (e) 3 VDC was applied for 2 h; (f) the filament was rinsed with DI water and then methanol; (g) finally the gold-plated filament was dried at 60 °C before further use. Two such filaments (complete with the bases) were inserted, oppositely oriented, into two end caps machined from G-PTFE with a 40 mm glass tube (10 mm i.d., 12 mm o.d.) providing the flow enclosure. Each end

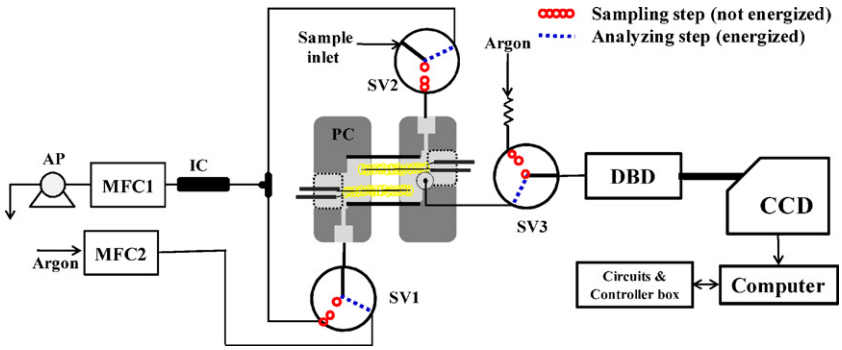

Fig. 1. System schematic. AP: air pump, MFC: mass flow controllers, IC: iodized charcoal, SV1–SV3: solenoid valves (driven together), PC: preconcentration chamber, DBD: dielectric barrier discharge cell, CCD: charge coupled device array spectrometer (other detectors were also used as indicated in text).

cap was provided with 1/4-28 threaded apertures for gas in/out connections through the preconcentration cell; one end cap has two such apertures (*vide infra*) and the other just one. The lamp base was sealed in place by hot-melt adhesive and the glass tube was sealed into the G-PTFE holders with PTFE tape. For desorption, 9 V was applied to the filaments in parallel for 15 s via a relay (JW2SN, www.digikey.com) actuated through one of the digital outputs.

2.4. General experimental setup

This is shown schematically in Fig. 1 and a photograph appears in Fig. S3. We make use of three 3-way all-fluorocarbon solenoid valves (SV1-3, 648K031, 12 VDC, www.Nresearch.com) configured as indicated. The instrument alternates between two modes in a cycle, the sampling mode and the measurement mode. It is desirable that SV1-SV3 (actuated in parallel) be driven in an energy-efficient configuration (especially in field use). The valve-port identities were therefore changed depending on whether the sampling period (t_s) was longer than the measurement period (t_m) or *vice-versa*. The configuration shown in Fig. 1 is for background sampling where $t_s > t_m$. During t_s the valves are not energized; the air sample or calibrant enters through SV2, is directed to the preconcentration chamber, and flows through the preconcentrator, through SV1, through a short cartridge (0.375″ o.d., 0.31″ i.d., 6 cm long) filled with pelletized iodized charcoal (05123, Fluka) to trap any residual mercury (needed only when high calibration concentrations are sampled) and then through the sampling mass flow controller MFC1 (Tylan FC 280, 10 standard liters per min) (SLM, all smaller gas flow rates are given in standard cubic centimeters per min (sccm)) (www.brooksinstrument.com) with the aspiration provided by an air suction pump AP (DOA-P120-FB, www.Gastmfg.com). A small flow of Argon, ~15 sccm, is meanwhile maintained by a restrictor orifice from a pressure regulated Ar cylinder source through SV3 into the DBD cell. During the measurement stage, all three valves are energized simultaneously through a MOSFET switch controlled by one of the digital outputs from the control computer. The sample now goes directly into the iodized charcoal column (this is only necessary when calibrating, to maintain constant flow conditions on the calibration source; for a real air sampling situation, the air sampling pump is shut off via a relay). Argon, flow rate controlled by MFC2 (UNIT UFC-1000, 1 SLM, www.Siemens.com) flows through SV1, through the preconcentration chamber and through the port connected to SV3 into the DBD and out. After air is completely removed from the preconcentration chamber, the preconcentration filaments are briefly heated and the desorbed Hg flows into the DBD cell and the resulting emission is detected. The sequence of events is provided in a tabular form in Table S1 in SI. When sampling ambient air, a 47 mm PTFE particulate filter (0.5 μm pore size) was used in the sample inlet to remove particulate matter.

3. Results and discussion

3.1. Effect of the plasma potential and plasma gas flow rate

The mercury spectral response relative to the background appears in the previous papers and is also given in Fig. S4. Initial ignition voltages for Ar and N_2 plasmas were 1.5 and 4.5 kV, respectively. The maximum voltage that could be safely applied before sparking occurred was 8.0 kV and sometimes resulted in cracked glass plates. Below this voltage and over a significant plasma gas flow rate range (88–439 sccm), the heat generated by the plasma was minimal. Fig. 2 shows the change in S/N (94 ng/L Hg), for both plasmas as a function of applied voltage (all of the signal was obtained by the Ocean Optics QE65000). While both plasmas show an increase in S/N with applied voltage finally reaching a plateau value, this plateau was reached at a lower applied voltage for the N_2 plasma than for the Ar plasma. The plateau S/N value was comparable in the two cases. In case of N_2, the S/N ratio reached a plateau by ~5.5 kV as one of the N_2 emission lines is close to the Hg emission line. Increasing the applied potential beyond this point increased both the Hg signal and plasma background in a manner that no further gain in S/N resulted. For Ar, the maximum S/N was observed at the maximum applied voltage that the plasma could be indefinitely operated in.

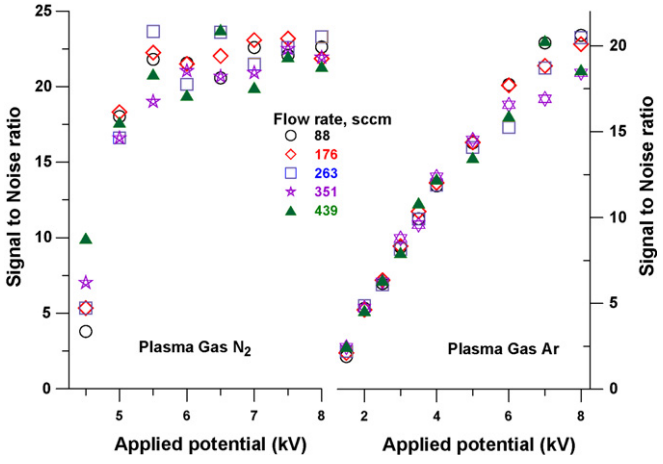

Fig. 2. Signal to noise ratio as a function of plasma gas flow rate and applied voltage for N_2 and Ar plasma gas, 23.5 pg Hg in DBD cell. Ocean Optics QE65000 detector. Spectra were acquired with 100 ms integration times. All spectra acquired over 60 s were averaged.

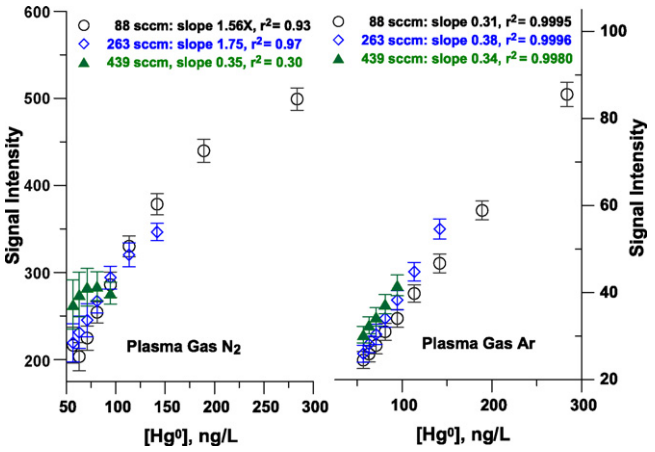

Fig. 3. Response behavior in N_2 and Ar plasma from ~50 to 300 ng/L. As flow rate is increased, source limitations limit the attainable high end concentration. These and data for all subsequent figures were obtained by the Hamamatsu C9404CA CCD spectrometer, 100 ms integration time. All spectra acquired over 60 s were averaged.

3.2. Response behavior

The response of the system to varying mercury concentrations for both the plasma types (N_2 and Ar plasmas, respectively, operated at 5.5 and 8 kV) is shown in Fig. 3. The absolute signal was much higher in the N_2 plasma but the standard deviation was also much higher. Perhaps more importantly, the signal was nonlinear with concentration and showed significant dependence on the flow rate. In contrast, the Ar plasma showed linear response up to high Hg concentrations at all gas flow rates. Therefore, the Ar plasma operated at 8.0 kV was used for further work.

3.3. Sensitivity comparison of different detectors

We tested several types of detectors to check their performance for the present purpose. Three CCD-array detectors (USB2000 and QE65000, both from www.oceanoptics.com and C9404CA, www.hamamatsu.com, the last two use high-sensitivity back-thinned CCDs) were equipped with their own monochromators and connected via optical fibers. The last two use 1024-element detector arrays, the USB 2000 uses a 2048 element array. Other detectors used were a head-on phototube (R6800U-01) and photomultiplier tubes (R7400U-09, H5784-06) all from www.hamamatsu.com; these were used with a modified end cap that allowed the placement of a narrow bandpass (half bandwidth 12 nm) high transmittance (>65%) interference filter centered at 254 nm (MaxLamp™ Hg01-254-25, www.semrock.com) ahead of the head-on photo (multiplier) tube. The arrangement is shown in Fig. S5 in SI. The results are shown in Table 1. Note that the integration times for the CCDs were 100 ms as opposed to 1 s for the photo(multiplier)tubes. The unamplified phototube did not sense any light either for the background plasma or in the presence of Hg. The solar blind photomultiplier tube provided 2× better S/N than the H5784 PMT sensor module. The H5784 responds to visible light as well and the interference filter is not completely opaque in the visible spectrum; as such, the background is much higher. In any case, neither of these PMTs were acceptable in this configuration to serve as detectors in trace Hg determination. The absolute light levels are low and it is a testament to current back-thinned CCDs that they can substantially outperform the PMT's. However, it is of course possible to use PMTs if, rather than using inefficient optical fibers, the light is gathered with more efficient collection optics and a high resolution monochromator is used to selectively detect the mercury line [17].

Of the CCD spectrometers, the low-cost USB-2000 spectrometer did not really provide enough sensitivity to perform trace analysis. The Hamamatsu CCD spectrometer showed the best performance with the highest S/N ratio (~60× better than the USB-2000) and was used for further work. Note that in the actual deployment with the preconcentrator, individual spectra with 100 ms integration time are taken over the 25 s period (see Table S1 in SI) after the filament is flash heated and these spectra are summed for the final result. The resulting S/N is of course much better than that taken for a single 100 ms run reported in Table 1.

3.4. Electrode area and placement

Different shapes and sizes of the electrode and its placement were investigated. Rectangular electrodes occupying or exceeding the entire channel width were found to be the best. Foil lengths of 10–50 mm were studied, 30–50 mm was found to produce the best and essentially the same result. Electrode placement was then optimized and ~10 mm from the exit was found to be the best position. Details are provided in Figs. S6 and S7 in SI.

3.5. Desorption voltage and time

Initial experiments were conducted by applying power to the filaments for a fixed time (30 s) and varying the applied voltage. At ≥12 V, some evaporation of gold from the filament was observed. The voltage was now systematically decreased; no difference in

Table 1
Relative performance of different detection systems[a].

Detector	Operating range	Slits and resolution	Operating conditions	Sample	Counts/100 ms (sd)	S/N
CCD spectrometer						
Hamamatsu C9404CA CCD	200–400 nm	140 μm, 3 nm	100 ms integration	Blank	1164 (19)	31
				82.7 ng/L Hg^0	2860(55)	
Ocean Optics QE6500 CCD	200–1100 nm	25 μm, 2.6 nm	100 ms integration	Blank	2460 (1.5)	17
				82.7 ng/L Hg^0	2494 (2.0)	
Ocean Optics USB2000 CCD	200–1100 nm	25 μm, 1.5 nm	100 ms integration	Blank	133.5 (2.3)	0.6
				82.7 ng/L Hg^0	134.9 (2.5)	
Detector	**Response range**	**Interference filter**	**Gain/power**	**Sample**	**mV (sd)**	***S/N***
Photo(multiplier) tube						
Hamamatsu PMT R7400U-09	160–320 nm	12 nm halfwidth	−850 V applied 1 s integration[b]	Blank	89.6 (6)	1.2
				82.7 ng/L Hg^0	96.5 (4)	
Hamamatsu PMT module H5784-06	185–650 nm	12 nm halfwidth	Gain control 0.85 V, 1 s integr.[b]	Blank	403 (5)	0.5
				82.7 ng/L Hg^0	398(9)	
Hamamatsu PT R6800U-01	185–320 nm	12 nm halfwidth	−15 V applied, 1 s integration	Blank	No light detected	*NA*
				82.7 ng/L Hg^0	No light detected	

[a] Ar flow rate 88 sccm, 8.0 kV Ar plasma.
[b] At these applied voltages both of these PMT's are operating with a radiant sensitivity of ~7×10^4 A/W, ~35% of maximum gain for the detector.

the signal was observed between 9 and 12 V applied. The powered interval duration was then decreased and down to at least 15 s, there was no change in the signal. This was considered a short enough time to provide long filament life.

3.6. Argon flush flow rate during desorption step

These experiments were conducted to determine the effect of the Ar flow rate during the desorption step and on carrying the desorbed mercury to the detector. A sample containing 0.73 ng/L mercury was preconcentrated for 1 min at 4.0 SLM. After sampling and switching of the solenoid valves, argon was allowed to flow through the preconcentration chamber and the DBD cell to completely displace the air (which would have shortened the life of the filaments when heated and would have disrupted excitation of Hg in the DBD cell) for some period before power was applied to the filaments. The flow rate had to be sufficient to sweep off the air in a reasonable period but not so high that the liberated Hg would be greatly diluted and argon use would be high. However, too low a flow rate would not only temporally broaden out the signal, it would also increase the time needed to flush the preconcentration chamber and thus increase analytical cycle time. We arbitrarily decided 2 min to be an acceptable period for the flushing step. The filament was heated for the next 15 s and the signal was recorded beginning at the time that power was applied to the filament (desorption and detection is complete within 30 s). Note that the Ar flow was continued for a further 3 min after the filaments were turned off even though signal acquisition was completed in a much shorter time. This allowed the filament to cool down and perform reproducible collection. This period may be lengthened if field measurements are conducted at a high ambient temperature. Fig. 4 shows the effect of varying the Argon flush flow rate between 90 and 440 sccm. There is a modest increase in the signal in going from 90 to 180 sccm (at which point the lowest relative standard deviation is reached). Beyond this flow there is no further significant gain in signal. We chose therefore a flush flow rate of 180 sccm for further work. The temporal signal profiles for various concentrations of Hg are shown in the inset of Fig. 4.

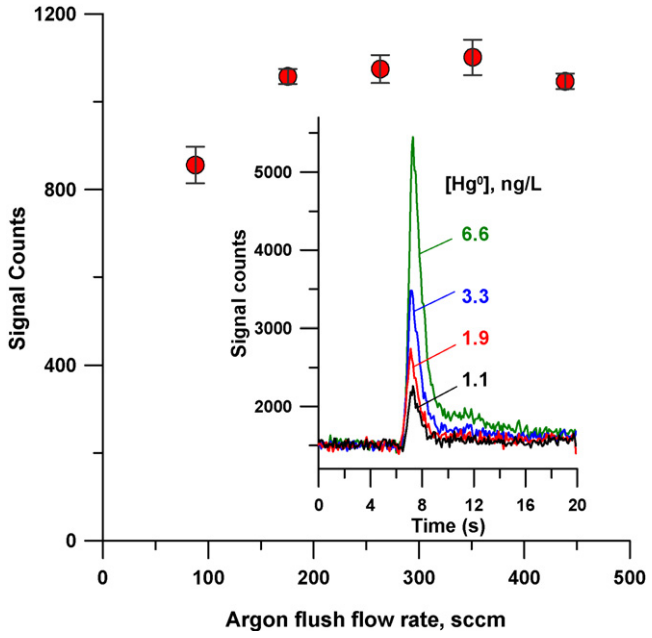

Fig. 4. Signal of 0.73 ng/L mercury (preconcentrated for 60 s at 4.0 SLM) at different argon flush flow rates. Inset shows signal profiles for 1.1–6.6 ng/L Hg preconcentrated at 0.88 SLM for 120 s, 180 sccm flush flow rate.

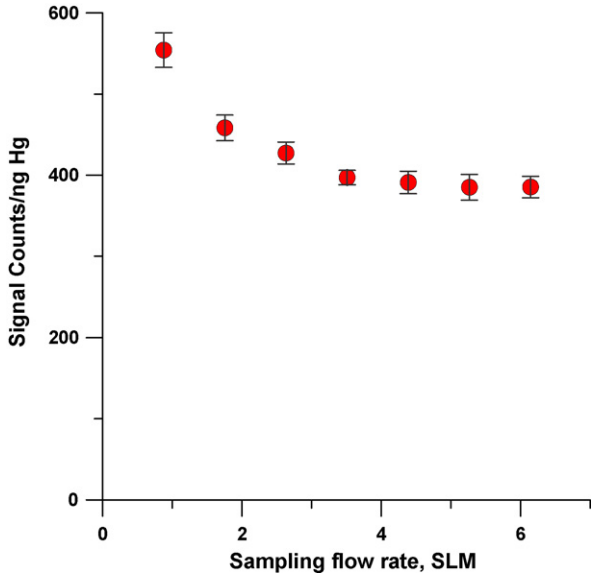

Fig. 5. The Hg signal response per unit amount of Hg as a function of sampling flow rate. The Hg concentration was 0.64 ng/L with a sampling time of 30 s.

3.7. Sampling rate during preconcentration

The influence of the sampling flow rate on the sensitivity was studied with a test Hg concentration of 0.73 ng/L preconcentrated for 30 s. A sampling rate much below 1 SLM would be impractical to measure trace concentrations while present system flow restriction limited the upper sampling rate to ~7 L/min. Experiments were conducted for sampling rates of 0.88–6.14 L/min. The dependence of the response per unit amount of mercury sampled on the sampling flow rate is shown in Fig. 5. In a simple tubular system, the collection efficiency monotonically decreases with flow rate [24]. The geometry of the present preconcentrator is such that purely laminar flow is extremely unlikely. Quantitative collection is not a prerequisite but reproducible collection is. We have not made an effort to evaluate the absolute collection efficiency in this work but obviously an appreciable fraction is collected even at the high end of the above sampling rate regime.

3.8. Repeatability and limit of detection

A four-point calibration experiment plus blank (0–6.6 ng/L), sampling 0.88 SLM for 120 s, was set up and conducted in triplicate at each point. A total of 19 such calibrations were repeated in an automated fashion over a 7-consecutive-day period. The calibration equation for the combined data was:

$$\text{signal counts} = 557(\pm 4.8)[\text{Hg}^0], \text{ng/L} + 56.8(\pm 18.2)$$

The relative standard error of the calibration slope was less than 1%, indicating the robustness of the technique, detailed data are shown in Fig. S8. The standard deviation of the responses at individual concentration points varied from 2.8 to 4.9%. Given the signal magnitude of the lowest concentration for this flow rate and this sampling period and the uncertainty of the blank measured under these same conditions, we calculate a limit of detection of 0.12 ng/L based on the three standard deviations over blank criterion. Note however, this only applies to these sampling conditions.

3.9. Dependence on humidity in direct measurement

The dependence of the emission signal on humidity has been previously noted for dry and water saturated conditions [17] but a

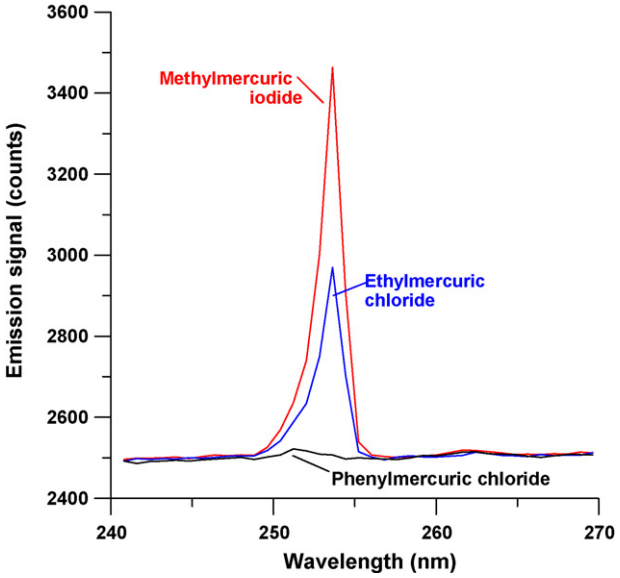

Fig. 6. Response of organomercurials when saturated headspace vapor over the solids in injected into the DBD-discharge.

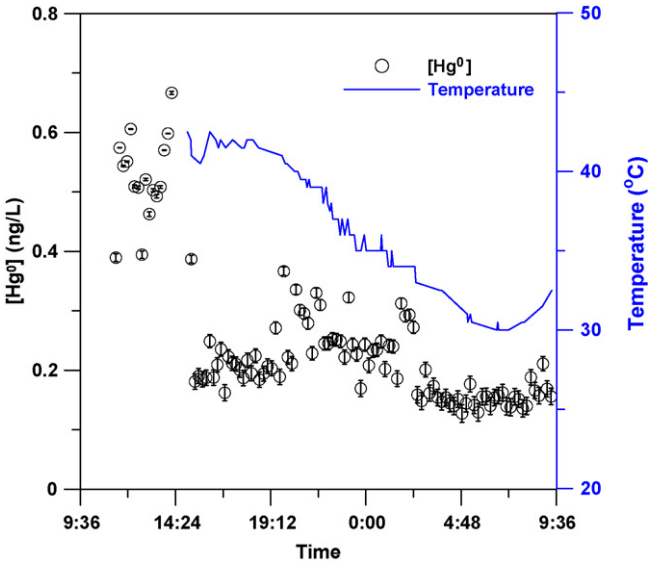

Fig. 7. Results of summertime continuous mercury measurement at a fluorescent lamp storage location at the University of Texas at Arlington. The temperature at the measurement location is also shown. The error bars shown in this and the next figure are not measurement uncertainties but represent the uncertainty associated with the calibration equation.

systematic variation was not conducted. Such an experiment shows that at humidities below 30% RH have little influence on the signal but the signal decreases dramatically above ~35% RH. While detailed data are shown in Fig. S9 in SI, this indicates that even if preconcentration is not needed for purposes of sensitivity, direct measurement results will be affected by ambient humidity. Preconcentration eliminates this issue and provides matrix isolation.

3.10. Response to organic mercury

It is of interest to determine if the system responds to organic mercury compounds, notably if the discharge is able to decompose organic mercury compounds. We tested methylmercuric iodide (mp 143 °C), ethylmercuric chloride (mp 193 °C) and phenylmercuric chloride (mp 251 °C) at high concentrations. The results are shown in Fig. 6. The specific concentrations of these compounds are unknown; the headspace vapor over the solid at ambient temperature was injected into the system. The fact that response is observed from MeHgI and EtHgCl (the response decreasing in order of increasing melting points) but not PhHgCl suggests that (a) the discharge is able to break the Hg-aliphatic C bond and (b) the vapor pressure of PhHgCl is too low for it to be measured this way and/or the Hg-aromatic C bond is more difficult to break. As organomercury compounds are not taken up by gold, speciation by initial removal of elemental Hg by gold followed by DBD measurement with or without preconcentration on gold (after photodecomposition, as is carried out for organoarsenicals [25]) will be possible. DBD-based direct selective detection of mercurials will be possible after chromatographic separation.

3.11. Field application

We used the instrument to measure the gas phase mercury in concentration in the fluorescent lamp recycling area of the University's environmental health and safety department in the summer of 2009. A sampling rate of 2.64 SLM was used with a sampling time of 5 min. The ambient temperature in the shed was also measured. The results are shown in Fig. 7. The instrument location was near the door of the shed where it was affected both by the outside wind and emissions from the storage area. Initially the concentration was high as the mercury had accumulated in the air. This concentration decreased abruptly as a breeze started in the mid-afternoon and the temperature started dropping down. The wind died down at midnight and the mercury levels then closely followed the temperature profile.

A second experiment was conducted at a lamp recycling plant. The sampling rate was as above, except 30 s preconcentration was used. In consultation with plant personnel, the instrument was deployed in the plant over a 24 h period. The air handling system is shut down after work hours; Fig. 8 shows that the mercury concentration rises remarkably in the enclosed area.

In summary, the gold-on-tungsten filament preconcentrator coupled with a DBD emission detector provides an excellent means

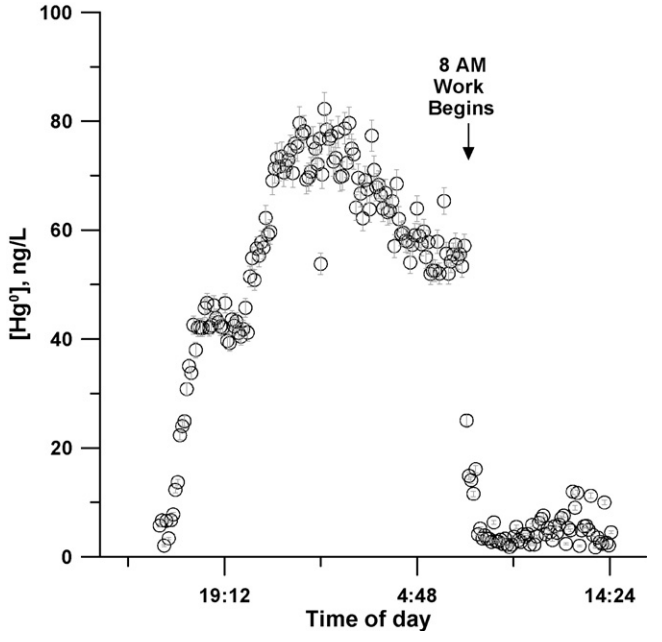

Fig. 8. Gaseous mercury concentrations in the air at a fluorescent lamp recycling plant. The air sample was collected at 2.64 SLM for 30 s. Note that mercury concentration drops abruptly as work begins and air handlers are started.

to make gaseous mercury measurements in a small footprint. The system is easily automated and provides high reproducibility.

Acknowledgments

This research was supported in part by the US National Foundation grant CHE-0821969 and Natural Science Foundation of China Major International Joint Research Project 20821120292. MP would like to acknowledge the financial support from the Thailand Research Fund through the Royal Golden Jubilee Ph.D. Program (Grant PHD/37/2550). We thank Ramon Ruiz, Environmental Health & Safety office, UTA and the Environmental Light Recyclers, Inc, Ft. Worth, TX and Dr. Martina Kroll for editorial assistance.

Appendix A. Supplementary data

Supplementary data associated with this article can be found, in the online version, at doi:10.1016/j.talanta.2010.02.005.

References

[1] M. Rose, M. Knaggs, L. Owen, M. Baxter, J. Anal. Atom. Spectrom. 16 (2001) 1101–1106.
[2] W.L. Clevenger, B.W. Smith, J.D. Winefordner, Crit. Rev. Anal. Chem. 27 (1997) 1–26.
[3] P. Kubáň, P. Houserová, P. Kubáň, P.C. Hauser, V. Kubáň, Electrophoresis 28 (2007) 58–68.
[4] J.Y. Lu, W.H. Schroeder, Water Air Soil Pollut. 112 (1999) 279–295.
[5] R. Puk, J.H. Weber, Appl. Organomet. Chem. 8 (1994) 293–302.
[6] S. Shimomura, Anal. Sci. 5 (1989) 633–639.
[7] C.J. Lin, S.O. Pehkonen, Atmos. Environ. 33 (1999) 2067–2079.
[8] R. Renner, Environ. Sci. Technol. 38 (2004) 448A–449A.
[9] B. Toole-O'Neil, S.J. Tewalt, R.B. Finkelman, D.J. Akers, Fuel 78 (1999) 47–54.
[10] J.J. McNerney, P.R. Busek, R.C. Henson, Science 178 (1972) 611–612.
[11] J.J. McNerney, Sensors 3 (1986) 39–41.
[12] W.A. Telliard, U.S. Environmental Protection Agency Method 245.7, http://www.epa.gov/waterscience/methods/method/files/245_7.pdf (accessed December 21, 2009).
[13] J.C.A. de Wuilloud, R.G. Wuilloud, M.F. Silva, R.A. Olsina, L.D. Martinez, Spectrochim. Acta B 57 (2002) 365–374.
[14] U. Engel, A.M. Bilgic, O. Haase, E. Voges, J.A.C. Broekaert, Anal. Chem. 72 (2000) 193–197.
[15] R. Martinez, R. Pereiro, A. Sanz-Medel, N. Bordel, Fresen. Z. Anal. Chem. 371 (2001) 746–752.
[16] Y.L. Yu, Z. Du, M.L. Chen, J.H. Wang, Angew. Chem. Int. Ed. 47 (2008) 7909-.
[17] Z.L. Zhu, G.C.Y. Chan, S.J. Ray, X.R. Zhang, G.M. Hieftje, Anal. Chem. 80 (2008) 8622–8627.
[18] B. Eliasson, W. Egli, U. Kogelschatz, Pure Appl. Chem. 66 (1994) 1275–1286.
[19] W.F. Fitzgerald, G.A. Gill, Anal. Chem. 51 (1979) 1714-.
[20] Z. Yoshida, K. Motojima, Anal. Chim. Acta 106 (1979) 405–410.
[21] G. Sallsten, K. Nolkrantz, Analyst 123 (1998) 665–668.
[22] T. Larsson, W. Frech, E. Bjorn, B. Dybdahl, Analyst 132 (2007) 579–586.
[23] Y.K. Inaba, T. Kawanobe, US Patent 3,993,808 (November, 1976).
[24] K. Toda, P.K. Dasgupta, Compr. Anal. Chem. 54 (2008) 639–683.
[25] A. Idowu, P.K. Dasgupta, Anal. Chem. 79 (2007) 9197–9204.